Cold atoms passing through a thin laser beam: a Fourier optics approach

Shuyu Zhou (周蜀渝)[1,2,*], Jun Qian (钱 军)[1], Shanchao Zhang (张善超)[2], and Yuzhu Wang (王育竹)[1,]**

[1]*Key Laboratory for Quantum Optics, Shanghai Institute of Optics and Fine Mechanics, Chinese Academy of Sciences, Shanghai 201800, China*

[2]*Department of Physics, The Hong Kong University of Science and Technology, Clear Water Bay, Kowloon, Hong Kong, 999077, China*

**Corresponding author: syz@siom.ac.cn; **corresponding author: yzwang@mail.shcnc.ac.cn*

Received January 29, 2016; accepted May 5, 2016; posted online June 13, 2016

A Fourier optics approach can be a concise and powerful tool to solve problems in atom optics. In this report, we adopt it to investigate the kinetic behavior of cold atoms passing through a far red-detuned Gaussian beam. We demonstrate that the aberration has significant influence on the evolution of the atomic cloud, which is rooted in the deviation of the Gaussian profile from the quadratic form. In particular, we observe an intriguing effect analogous to Fresnel's double prism with cold atoms. The experimental results are in good agreement with the numerical simulation.

OCIS codes: 020.1335, 020.3320, 070.7345.
doi: 10.3788/COL201614.070202.

Atoms have wave-particle duality[1,2]. However, the wavelength of the thermal de Broglie wave of hot atoms is so short that their kinetic problems can be dealt with using the approaches developed for classical particles[3,4]. With the rapid development of atom cooling techniques, atomic samples with the temperature of several micro Kelvins were achieved by using laser cooling[5–9]. They can be further cooled via evaporative cooling[10,11] and prepared as ultracold atoms or Bose–Einstein condensates (BECs) with temperatures of nano-Kelvins[12,13]. Ultracold atoms have longer thermal de Broglie wavelengths and exhibit more significant wave properties, such as interference and diffraction[14–17], so, the kinetic problems of ultracold atoms should be addressed in a wave picture. The path-integral approach, which can give strict solutions to kinetic problems where the wave properties need to be considered, has been developed[18–20]. However, it is technically complicated and not intuitive.

In this Letter, we propose a simple approach to handling this kind of problem. Some results in geometric optics should be reproduced in Fourier optics when the interference and diffraction can be neglected[21,22]. Naturally, the Fourier optic approach can be used to solve problems in atom optics, such as the transport of atomic clouds in optical potentials. Here we derive the effective focal length of a quadratic and a Gaussian beam. In the former case, the potential is equivalent to an ideal atomic lens. Then we discuss the case in which the Gaussian potential cannot be approximated as a quadratic potential. When a spherical atomic cloud passes through a far-detuned Gaussian laser beam, a novel effect analog of a light beam passing through a Fresnel's double prism is observed.

Classically, for a light wave propagating in a medium with refractive index $n(\vec{r})$, the wave vector is

$$\vec{k}(\vec{r}) = \frac{2\pi n(\vec{r})}{\lambda_0}\vec{k}, \tag{1}$$

where λ_0 is the wavelength of light in a vacuum and $\vec{k}_0$ is the unit vector pointing in the direction of the maximum light-phase gradient. However, for an atom moving in a potential well, one can update the wave vector with

$$\vec{k}(\vec{r}) = \sqrt{\frac{2M[E - V(\vec{r})]}{\hbar^2}}\vec{k}_0, \tag{2}$$

where E is the total atomic energy and $V(\vec{r})$ is the potential. Given that the wave vector of a free particle is $\sqrt{2ME/\hbar^2}\vec{k}_0$ in the de Broglie relation, the effective refractive index of the potential can be expressed as

$$n(\vec{r}) = \sqrt{1 - V(\vec{r})/E}. \tag{3}$$

This equation also can be obtained by comparing the basic function in geometric optics (eikonal equation) with the Jacobi–Hamilton equation[21,23]. When $|V| \ll E$,

$$n(\vec{r}) \approx 1 - \frac{V(\vec{r})}{2E}. \tag{4}$$

For simplicity, we begin with a cylindrical atomic lens. Here, we assume that the atomic lens is constituted by a one-dimensional harmonic potential in the x direction, which is independent of its position in the z direction. The potential is given by

$$V(x, z) = \frac{\kappa}{2}x^2, \tag{5}$$

where κ is a constant. Then, we have

$$n-1=-\frac{\kappa x^2}{4E}. \tag{6}$$

We assume that the potential only exists between 0 to h in the z direction, and the equivalent optical length is

$$\int_0^h (n-1)\mathrm{d}z=-\frac{\kappa x^2 h}{4E}. \tag{7}$$

The phase transfer function of an ideal cylindrical lens is

$$\varphi=-\frac{x^2 k}{2f}, \tag{8}$$

where f is the focal length. Comparing Eq. (7) with Eq. (8) yields

$$f=\frac{2E}{\kappa h}. \tag{9}$$

Now, we focus on the situation where the atomic lens is built by a red-detuned Gaussian beam, whose potential is:

$$U(x,z)=U_0 e^{-\frac{x^2}{2\sigma_x^2}-\frac{z^2}{2\sigma_z^2}}, \tag{10}$$

$$U_0=U(0,0)\approx\frac{\hbar\Omega^2(0,0)}{4\delta}, \tag{11}$$

$$\Omega=\Gamma\sqrt{\frac{I}{2I_s}}, \tag{12}$$

where δ is the detuning of the laser field from the atomic resonance. Γ is the natural decay rate of the excited state, which is $2\pi\times 5.75$ MHz for the ^{87}Rb D1 ($5^2S_{1/2}\rightarrow 5^2P_{3/2}$) transition. I_s is the saturation intensity, which is 4.48 mW/cm^2 for a π-polarized light field that is far detuned from the D1 line. Therefore, we have

$$n\approx 1-\frac{U}{2E}=1-\frac{\hbar\Omega^2(0,0)e^{-\frac{x^2}{2\sigma_x^2}-\frac{z^2}{2\sigma_z^2}}}{8E\delta}, \tag{13}$$

where E is the incident kinetic energy. Then, the integral of n in the z direction is

$$\int n\mathrm{d}z\approx A+Be^{-\frac{x^2}{2\sigma_x^2}}, \tag{14}$$

$$B=\frac{\sqrt{2\pi}\hbar\Omega^2(0,0)\sigma_z}{8E|\delta|}. \tag{15}$$

The Gaussian function can be expanded as a power series:

$$e^{-\frac{x^2}{2\sigma_x^2}}\approx 1-\frac{x^2}{2\sigma_x^2}. \tag{16}$$

Consequently, the optical length is $-\frac{x^2 B}{2\sigma_x^2}$, and the amplitude transmissivity is

$$\tilde{t}_{\mathrm{atom}}(x)=\exp\left(-ik\frac{x^2 B}{2\sigma_x^2}\right). \tag{17}$$

Compared with the amplitude transmissivity of a thin lens

$$\tilde{t}_{\mathrm{lens}}(x)=\exp\left(-ik\frac{x^2}{2F}\right), \tag{18}$$

we obtain the focal length as

$$F=\frac{\sigma_x^2}{B}=\frac{4mv^2|\delta|\sigma_x^2}{\sqrt{2\pi}\hbar\Omega^2(0,0)\sigma_z}. \tag{19}$$

The same result can be derived from Newtonian mechanics[24].

Although a Fourier optics approach is a general method, the most convenient application is to calculate the diffraction of a plane. Therefore, it is particularly suitable for the case that external fields only imprint a spatial phase distribution on the wavefront but do not change the atomic density distribution. We also notice that in an ultracold atomic cloud with a very high density ($\sim 10^{13}$/cm^3, BECs in traps can reach it), the interactions between atoms could break the validity of the Fourier optics method. Fortunately, once the atomic clouds are released from the trap, their density will decline rapidly. After several milliseconds of ballistic expansion, the effect of the interaction between the atoms can be ignored. So the Fourier optics approach is valid under most of the experimental conditions.

The schematic of our experiment is depicted in Fig. 1. We load a cold atomic cloud into a quadrupole-Ioffe configuration (QUIC) trap with trap frequencies $(\omega_x,\omega_y,\omega_z)=2\pi\times(210,21,210)$ Hz. Then, we lower the temperature of the atoms by RF-induced evaporative cooling. The final temperature can be tuned from about 1 μK to below the Bose–Einstein transition temperature by setting different final RF frequencies[25]. Both the Gaussian beam and the probe beam are located below the center of the QUIC trap and propagate parallel to the long axis of this trap. The focused Gaussian beam overlaps the center of the atomic cloud after being released from the QUIC trap for 7 ms. In the z direction, the atoms are confined in a region that is less than 10 μm initially. The cold atomic cloud ballistically expands after the magnetic trap is switched off. We acquire the distribution of atomic clouds from the absorption images. The wavelength of the laser for the atomic lens is about 795 nm, with $2\pi\times$ 50 GHz red detuned from the transition of the D1 line. The waist size of the Gaussian beam is $w_0=2\sigma_0\approx$ 46 μm, and the Rayleigh length is about 8.5 mm. The laser beam provides a two-dimensional Gaussian potential because the Rayleigh length is far larger than the atomic cloud. The power of the Gaussian beam is about 45 μW, and the Rabi frequency is $\Omega=2\pi\times 71$ MHz. The wavelength of the probe laser is about 780 nm and tuned to the $F=2\rightarrow F=3$ transition of the D2 line. A narrowband filter that is transparent at 780 nm and opaque at 795 nm is inserted into the imaging path. The imaging

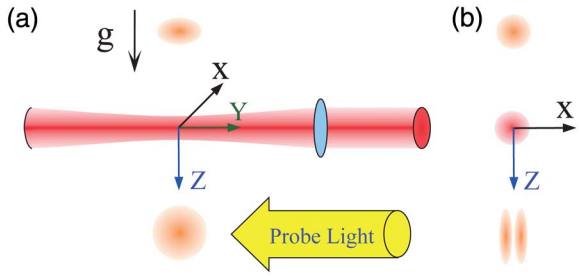

Fig. 1. (a) Schematic of experimental setup. A cold atomic cloud interacts with a red-detuned Gaussian beam under gravity. A probe beam propagates along the y-axis for the absorption images. (b) A side view of the experiment.

system consists of a battery of lenses with the diffraction limit of 3 μm. However, the real resolution is about 10 μm due to residual aberrations.

In our previous work, we observed several exotic phenomena such as the focusing and advancement of atomic clouds after they passed through a far red-detuned Gaussian beam. We did numerical simulations via the direct-simulation Monte Carlo approach for thermal atomic clouds and the non-linear Schrödinger equation for BECs[25]. A theoretical investigation of the one-dimensional focusing of cold atomic clouds based on Newtonian mechanics was also performed[24]. Although all these were consistent with experimental results, they did not provide an intuitive physical picture. Now we try to understand the nature of these experiments via a different approach.

In the preceding discussion, we obtained the expression of the focal length of a Gaussian beam under the approximation of $x \ll \sigma$. It is valid only when the size of the atomic cloud is much smaller than the width of the Gaussian beam (the paraxial approximation). In practice, however, the size of the atomic cloud is often comparable to or even larger than that of the Gaussian beam. Higher order polynomial expansion of the Gaussian potential will bring aberrations. A Gaussian function has the maximum of curvature at its center and decreases toward the wings. Therefore, the different x positions of the Gaussian beam have different focus lengths. In our previous work, we have pointed out that this kind of the aberration induces a collimation effect of the atoms along the x direction, which is valid for the initial parameters within a wide range[24,25]. Here, we explore this effect by imaging the atomic cloud after different flight intervals, as shown in Fig. 2. In Fig. 2(a), the atoms fly 7 ms after passing through the Gaussian beam. The position of the atomic cloud at this moment is very close to the calculated image point under the approximation of $x \ll \sigma$. A narrow peak emerged from the broadened background. In Figs. 2(b,c), after flying 9 and 13 ms, the widths of the central peaks only slightly vary although the image points change distinctly, which is also clearly illustrated in the density distributions of the atomic clouds along the x-axis (see Fig. 2(d)). The analysis based on atomic trajectory approach and the direct Monte Carlo simulation can be found in Refs. [24,25].

A smaller Gaussian beam could exhibit more remarkable effects. First, the smaller width of the Gaussian beam causes a shorter focal length, according to Eq. (19). It is helpful for observing the far-field effects with a finite flight time. Second, for the Gaussian beam with a smaller size, its wings overlap with more atoms and have non-ignorable contributions on the atomic movement. This benefits the exhibition of the aberration effects since the wings of the Gaussian beams cannot be approximated as quadratic potentials. In the following experiment, a remarkable splitting of the atomic cloud manifests the influence of the aberration induced by the Gaussian beam, which is similar to a plane light wave passing through Fresnel's double prism[21].

We carry out the experiment the same way as seen in Fig. 2, except the waist size of the Gaussian beam is chosen to be 28 μm. The power of the Gaussian beam is 24 μW, and the Rabi frequency is $\Omega = 2\pi \times 88$ MHz. The laser frequency was still $2\pi \times 50$ GHz red detuned from the transition of the D1 line.

Without the red-detuned Gaussian beam, the atomic cloud only exhibits a Gaussian profile while it flew 16 ms, as shown in Fig. 3(a). By turning on the Gaussian beam, as aforementioned, the distribution of the transmitted atomic cloud changes dramatically. Figures 3(b)–3(d) are the images of atomic clouds flying 1, 5, and 9 ms after they passing through the Gaussian beam, respectively. The black hole in Fig. 3(b) indicates the position of the

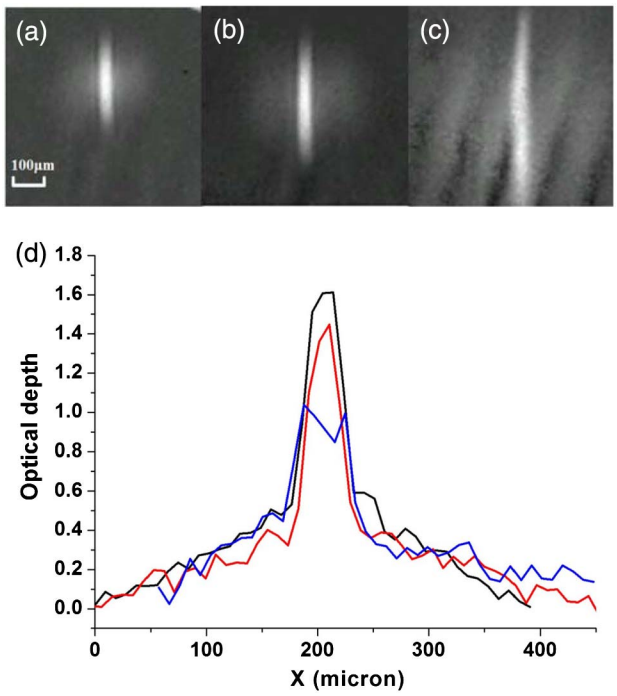

Fig. 2. Experimental results of cold atomic clouds passing through a Gaussian laser beam. (a)–(c) Images of atomic clouds flying 7, 9, and 13 ms after passing through the Gaussian beam, respectively. (d) The black, red, and blue lines are the cross curve of the optical depths of (a)–(c) along the x-axis at the widest part of the atomic clouds.

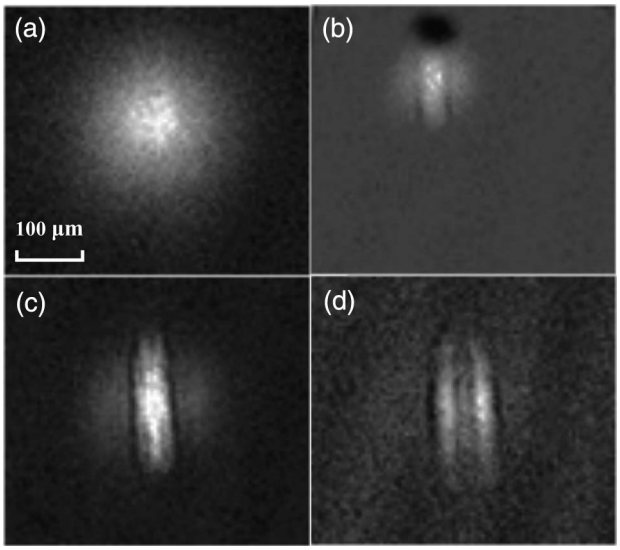

Fig. 3. Experimental results. (a) The atomic cloud ballistically expands 16 ms after being released from the QUIC trap. (b)−(d) Images of atomic clouds flying 1, 5, and 9 ms after passing through the Gaussian beam, respectively.

Gaussian beam. When the atomic cloud just penetrates the Gaussian beam, we can only find a high-density part in the center with a background. The image point was located at the place of the atomic cloud flying 1.8 ms after passing the laser beam. The focal length was obtained by using Eq. (19). As shown in Fig. 3(c), after a 5 ms flight, the central part of the atomic cloud still looked like a single peak. Remarkable splitting appears when the atoms experience a longer flight. Two narrow bands in the atomic cloud are obviously visible with a broadening background in Fig. 3(d). The image of a flight time of 9 ms clearly showed the image formation of the edge parts of the Gaussian beam. The atomic image-forming system with the wings of the Gaussian beam is approximately equivalent to two lenses placed at the two positions and a Fresnel's double prism superimposing with them.

Clearly, the thermal motion of atoms also gives rise to the aberration since the refractive index is dependent on the kinetic energy of the atoms (Eqs. (3) and (4)). Thus, we should cool the atoms to a very low temperature to alleviate the influence of the thermal motion. In our setup, for example, the temperature of the atomic cloud is about 600 nK, which is slightly higher than the Bose−Einstein transition temperature. In this situation, we estimate that the fluctuations of $(n-1)$ and the focal length are about ±4%. The fluctuation of the image distance is the same order as that of the focal length.

On the other hand, the time of flight imaging method is interestingly found to play an important role in selecting the velocity of atoms both in the longitudinal (z) direction and the transverse (x) direction. Given that the initial size of atomic clouds is very small, the positions of the atoms in the z direction after time of flight are determined by the initial velocity distribution of atoms. When we select the cross curves in the x direction that passes across the center of the atomic cloud in z direction, these atoms have very small initial velocities along the z-axis. The miniature size of the Gaussian beam also plays a role in the selection of the velocities of the atoms in the x direction. Atoms can interact with the Gaussian beam having the same velocity distribution even if the atomic clouds have different temperatures in the trap. This effect was clearly illustrated in Fig. 6 of Ref. [25]. Therefore, we can select the cross curves of the optical depth in the center of the atomic cloud to compare with the numerical simulation.

A numerical simulation has been conducted based on the Rayleigh−Sommerfeld formulation[21]:

$$U(p_0) = \iint_{\sum} h(p_0, p_1)\, U(p_1)\mathrm{d}S, \tag{20}$$

where $U(p_0)$ is the amplitude at the observation point p_0, and $U(p_1)$ is the amplitude at the initial wave front in the plane aperture $\sum$. The impulse response $h(p_0, p_1)$ is given by

$$h(p_0, p_1) = \frac{1}{i\lambda}\frac{e^{ikr_{01}}}{r_{01}}\cos(\vec{n}, \vec{r}_{01}), \tag{21}$$

where $\cos(\vec{n}, \vec{r}_{01})$ represents the cosine of the angle between the outward normal $\vec{n}$ of $\sum$ and vector $\vec{r}_{01}$ joining p_0 and p_1.

We assume that the phase factor of the atomic wave is the same as a spherical wave but the amplitude distribution is a Gaussian function. The amplitude transmissivity of the atomic wave is given by Eq. (17). Hence, the initial wave front $U(p_1)$ in $\sum$ is a product of the input atomic wave and the amplitude transmissivity. We assume that the depth of the atomic lens can be ignored, so the position of $\sum$ is in the center of the Gaussian beam. The effect of the gravitational field on the atoms should be considered. If the gravity field only exists in a slight layer containing the laser beam, it does not affect the characteristic of the atomic lens because the gravitational field adds the same phase factor over all the x coordinates. However, given that gravity exists in all the spaces, it should affect the propagation of the matter wave. In a previous work, we found that the equivalent object distance under gravity is twice the distance from center of the QUIC trap to the atomic lens[24]. In order to compare our simulation with experimental results under gravity, we study the motion of the atomic cloud in a special frame of reference once the atomic cloud arrives at the center of the Gaussian beam. This frame of reference moves with gravitational acceleration g, in which the atomic cloud moves at an approximately constant velocity in the z direction. The method is suitable for comparing the numerical analysis with the experimental results because the image distance is proportional to the flying time in this frame. Taking into account the finite-size effect of the atomic cloud, the final distribution of the atomic cloud is a superposition of all intensity distributions due to different atoms in the initial atomic cloud. We use an intensity superposition instead of an

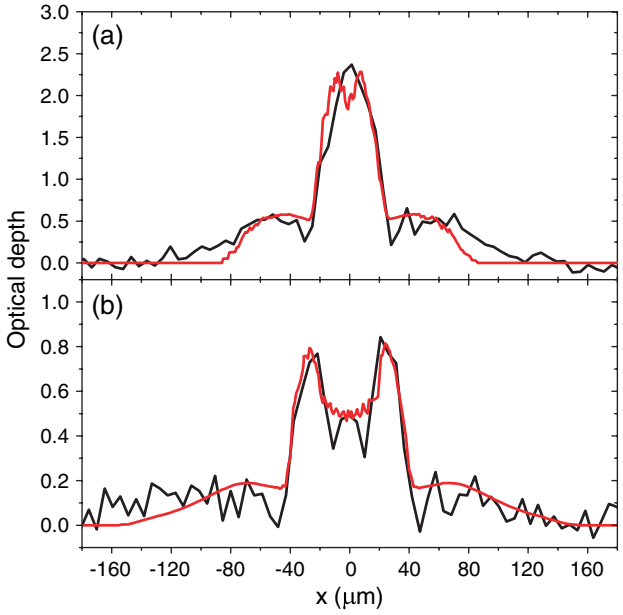

Fig. 4. (a) and (b) Cross curves of the optical depths in Figs. 3(c) and 3(d) (black lines) and numerical simulations (red lines).

amplitude superposition because the thermal de Broglie wavelength of the atoms is much less than the scale of the atomic cloud in our experiment. However, if we use BECs as atomic sources, we need to calculate the amplitude superposition. We find our calculations agree with the experimental data, as shown in Fig. 4. The black lines in Figs. 4(a) and 4(b) are the experimental results indicating the cross-sectional line of the atomic cloud along the x-axis taken at the widest part of the atomic clouds in Figs. 3(c) and 3(d). The red lines in Fig. 4 are the simulation results. All the simulation parameters are same as those in experiments. The small deviation between the experimental and numerical simulations is due to diffraction and aberration in the imaging system.

In conclusion, we use a Fourier optic method to investigate the behavior of a cold atomic cloud after passing through a thin red detuned laser beam. The focus length of a Gaussian beam is obtained under the approximation of a paraxial condition. We also study an effect similar to an atomic Fresnel's double prism when the paraxial approximation cannot be satisfied. Compared with the direct simulation Monte Carlo or path-integral methods, our approach is simple and comprehensible. It can be used to handle both coherent and incoherent atomic waves. These results may provide valuable insights in designing and manipulating the key ingredients of atom optics.

The authors thank Drs. Shengwang Du and Zhenglu Duan for the helpful discussions. This work was supported by the National Natural Science Foundation of China under Grant Nos. 10804115 and 91336103. Q. J. acknowledges the support by the National Natural Science Foundation of China (No. 11104292).

References

1. I. Estermann and O. Stern, Z. Phys. **61**, 95 (1930).
2. W. Greiner, *Quantum Mechanics: An Introduction* (Springer-Verlag, 2001).
3. J. J. McClelland and M. R. Scheinfein, J. Opt. Soc. Am. B **8**, 1974 (1991).
4. V. I. Balykin and V. G. Minogin, Phys. Rev. A **77**, 013601 (2008).
5. E. L. Raab, M. Prentiss, A. Cable, S. Chu, and D. E. Pritchard, Phys. Rev. Lett. **59**, 2631 (1987).
6. C. Monroe, W. Swann, H. Robinson, and C. Wieman, Phys. Rev. Lett. **65**, 1571 (1990).
7. P. D. Lett, W. D. Phillips, S. L. Rolston, C. E. Tanner, R. N. Watts, and C. I. Westbrook, J. Opt. Soc. Am. B **6**, 2084 (1989).
8. Z. Zhang, Z. Ji, Z. Li, J. Yuan, Y. Zhao, L. Xiao, and S. Jia, Chin. Opt. Lett. **13**, 110201 (2015).
9. B. Yang, J. Wang, and J. Wang, Chin. Opt. Lett. **14**, 040201 (2016).
10. K. B. Davis, M. O. Mewes, M. A. Joffe, M. R. Andrews, and W. Ketterle, Phys. Rev. Lett. **74**, 5202 (1995).
11. D. Xiong, P. Wang, Z. Fu, S. Chai, and J. Zhang, Chin. Opt. Lett. **8**, 627 (2010).
12. M. H. Anderson, J. R. Ensher, M. R. Matthews, C. E. Wieman, and E. A. Cornell, Science **269**, 198 (1995).
13. K. B. Davis, M. O. Mewes, M. R. Andrews, N. J. Van Druten, D. S. Durfee, D. M. Kurn, and W. Ketterle, Phys. Rev. Lett. **75**, 3969 (1995).
14. F. Shimizu, K. Shimizu, and H. Takuma, Phys. Rev. A **46**, R17(R) (1992).
15. M. R. Andrews, C. G. Townsend, H. J. Miesner, D. S. Durfee, D. M. Kurn, and W. Ketterle, Science **275**, 637 (1997).
16. Y. Hung, B. Schuller, J. Giblin, and J. Shertzer, Phys. Rev. A **73**, 062722 (2006).
17. S. W. Chiow, T. Kovachy, H. C. Chien, and M. A. Kasevich, Phys. Rev. Lett. **107**, 130403 (2011).
18. R. P. Feynman and A. R. Hibbs, *Quantum Mechanics and Path Integrals* (McGraw-Hill, 1965).
19. G. M. Gallatin and P. L. Gould, J. Opt. Soc. Am. B **8**, 502 (1991).
20. M. Gondran and A. Gondran, Am. J. Phys. **73**, 507 (2005).
21. M. Born and E. Wolf, *Principles of Optics*, 6th Ed (Cambridge University Press, 1997).
22. J. W. Goodman, *Introduction to Fourier Optics*, 2nd Ed (McGraw-Hill, 1996).
23. J. J. Sakurai, *Modern Quantum Mechanics* (Benjamin-Cummings Publishing, 1985).
24. Z. L. Duan, S. Y. Zhou, T. Hong, and Y. Z. Wang, arXiv:1108.3144v2 (2011).
25. S. Y. Zhou, Z. L. Duan, J. Qian, Z. Xu, W. P. Zhang, and Y. Z. Wang, Phys. Rev. A **80**, 033411 (2009).